
Scalable Computing: Practice and Experience, ISSN 1895-1767, http://www.scpe.org
© 2024 SCPE. Volume 25, Issues 6, pp. 5424–5430, DOI 10.12694/scpe.v25i6.3429

THE GARDEN VEGETATION COVERAGE MONITORING AND SPATIAL ANALYSIS MODEL BASED ON REMOTE SENSING TECHNOLOGY

YINGYING TAN* AND JIANG CHANG†

Abstract. A correlation study was conducted between SPOTVEGNDVI monthly data and rainfall data in Yulin, Yan 'an, Xi 'an and Ankang of Shaanxi Province from 2015 to 2022. The ecological effects of urban vegetation cover were studied using the revised standardized Vegetation Index (NDVIC). It is found that NDVIC has a strong correlation with precipitation, and its correlation increases with the increase of altitude. Vegetation cover in the Ankang area increased significantly from 2016 to 2022. The net primary productivity index of urban green space increased significantly in October 2016-2022, which is an objective reflection of the effectiveness of urban green construction. This study can lay a theoretical foundation for the objective quantitative assessment of the ecological effects of urban vegetation cover.

Key words: Garden vegetation cover; Revised standardized vegetation index (NDVIC); Pixel binary model; Precipitation

1. Introduction. Soil erosion and desertification are the most severe ecological problems in China. This is also the main reason for the frequent occurrence of flood disasters and wind and sand disasters in recent years [1]. Vegetation is critical in soil improvement, climate control, carbon dioxide emission reduction, soil and water conservation, and conservation. Remote sensing can make rapid and large-scale ground-to-ground observations non-contact, providing vital support and accuracy guarantees for large-scale and dynamic ecological environment monitoring. Using advanced remote sensing to monitor the vegetation evolution of forest ecosystems in real-time can shorten the time of field investigation, reduce the cost and improve monitoring accuracy. At the same time, it allows researchers to carry out real-time observation in areas that are difficult to access, such as mountains, deserts and wetlands. It is more practical. Presently, domestic and foreign researchers mainly use Landsat remote sensing and MODIS remote sensing images to study the vegetation coverage of the study area [2]. There are few studies on regional plant coverage based on satellite remote sensing data of Ankang City. Most of the current research is carried out in Shaanxi province. Reference [3] uses MODIS/NDVI data combined with meteorological and DEM data to study the temporal and spatial distribution characteristics of vegetation coverage in Shaanxi Province in recent years and discusses the effects of temperature and rainfall on vegetation coverage. Literature [4] uses a pixel dichotomous model to study the ecological environment of Buxell County. Literature [5] studied the ecosystem in the source area of the Kaidu River based on the binary model of image elements. Literature [6] used satellite image data to study the vegetation cover in the North Canal Zone. In literature [7], the pixel simulation method was applied to study the urban area of Kashgar, Xinjiang. Ecological environmental protection and biodiversity protection in Ankang City are the basis for evaluating the implementation effect of ecological engineering projects and environmental protection [8]. This project plans to take Yulin, Yan 'an, Xi 'an and Ankang in Shaanxi Province as the research objects [9]. In this paper, an improved standardized Vegetation index (NDVIC) is established to study the influence of vegetation cover on urban construction.

2. Overview of the survey area. Shaanxi Province is a severe soil and water loss and desertification area in China. The area of soil and water loss has reached 66.9%, which has seriously affected the region's economic development [10]. Through ecological and environmental protection projects such as afforestation, 60% of soil erosion has been eliminated by the end of 2019. Yulin (YL), Yan 'a (YA), Xi 'an (XA) and Ankang (AK) are located in the North-South transect of Shaanxi Province, and their natural conditions and precipitation have

*School of Modern Agriculture and Biotechnology, Ankang University, Ankang, Shaanxi, China, 725000 (Corresponding author, changjiang_009@163.com)
†School of Modern Agriculture and Biotechnology, Ankang University, Ankang, Shaanxi, China, 725000

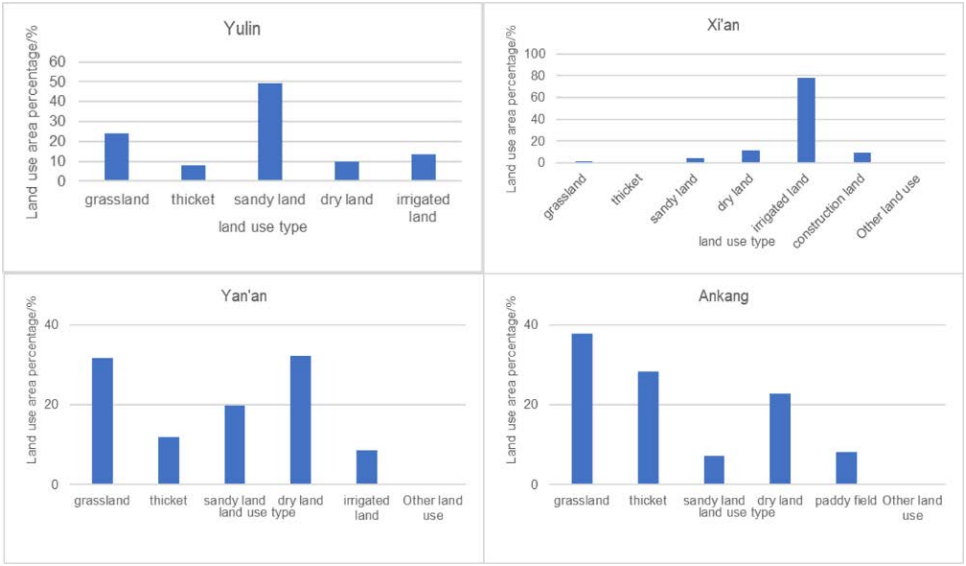

Fig. 2.1: *Land use status of Yulin, Yan 'an, Xi 'an and Ankang in 2017.*

a good transition, which is suitable for NDVI precipitation related research, and also show an excellent spatial pattern from north to south (fig. 2.1).

3. Data and methods.

3.1. Data Sources. In this paper, remote sensing images of 1 km*1 km were obtained from 2015 to December 31, 2022, using SPOT VEGETATION satellite data [11]. There are 300 images. Its calculation method is given in equation (3.1).

$$NDVI = \frac{NIR - \mathrm{Re}\, d}{NIR + \mathrm{Re}\, d}$$

NIR represents the reflectivity of SPOT in the red-light region. Red represents the wavelength of SPOT. NDVI ranges from 0.1 to 0.7. With the increase of NDVI value, vegetation coverage increased gradually. The NDVI of the study area is the average NDVI of each pixel [12]. The NDVI for that month is the average of the previous, middle and following three months of each month. The national precipitation data from 2015 to 2022 are the precipitation data of the China Meteorological Administration from 2015 to 2022. The rainfall of each month is the sum of the daily rainfall.

3.2. Establishment of Green Plant Coverage Evaluation Index system. The linear regression model of NDVI and precipitation is given by equation (3.2).

$$NDVI_R = f(R\alpha \text{ in fall }) = \alpha R + \beta$$
$$NDVI_C = NDVI_{ob} - NDVI_R$$

$NDVI_R$ is the monthly average $NDVI$ value obtained by the multiple linear regression model in the study area. R stands for precipitation intensity. α, β is a parameter of the equation. The $NDVI_C$ index of structure (3.3) is used to reflect the influence of urban green landscape. Where $NDVI_C$ is $NDVI$ after deducting rainfall response. $NDVI_{ob}$ is the objective, standardized vegetation index on the NDVI image.

3.3. Pixel binary mode. The basic idea of "pixel dichotomy" is to divide the reflection coefficient of the pixel S into two regions: reflectance S_α of the vegetation part and S_β of the non-vegetation part, in which the

reflectance of any pixel can be expressed by reflectance S_α of vegetation part and S_β of nonvegetation part, that is:

$$S = S_\alpha + S_\beta$$

Suppose that the proportion of one plant in each pixel on the image is g_z (the vegetation coverage on the pixel), then the proportion of the two types is $1 - g_z$. The reflectance of a pixel is S_{veg} when it is completely covered by plants, and S_{soil} when it is completely uncovered by vegetation. The information S_α contributed by the vegetation portion of the mixed pixel can be expressed as an integral on one pixel [13]. It is a pure product of vegetation reflection coefficient S_{veg} and pixel G_z. The information S_β contributed by non-vegetation components can be expressed as the product of S_{soil} and $1 - G_z$

$$S_\alpha = G_z \times S_{\text{veg}}$$
$$S_\beta = (1 - G_z) \times S_{\text{soil}}$$

By solving equations (3.4), (3.5) and (3.6), the following formula for calculating vegetation coverage can be obtained:

$$G_z = (S - S_{\text{soil}}) / (S_{\text{veg}} - S_{\text{soil}})$$

3.4. Extraction of vegetation coverage. This project selects the highest annual peak value of MODIS NDVI data as the vegetation cover data. According to the pixel dichotomy theory, it is assumed that surface NDVI can be divided into two components [14]. That is, the information contributed by the green vegetation part and the information contributed by the non-vegetated part. According to the method of formula (3.7), the calculation formula of "vegetation coverage" can be expressed as:

$$G_z = (NDVI - NDVI_{\text{soil}}) / (NDVI_{veg} - NDVI_{\text{soil}})$$

$NDVI_{\text{soil}}$ indicates the value of $NDVI$ for the area where the soil is entirely bare or without plants [15]. $NDVI_{\text{veg}}$ represents pixel $NDVI$ covered by plants, which is simply pixel $NDVI$. When there is no observation data, the minimum of NDVI of a specific confidence interval is used as the best non-vegetation coverage on the image of the evaluation area. is $NDVI_{\text{veg}}$ to select the maximum NDVI value on the evaluation area image of a specific trusted range, that is, the ideal vegetation coverage area of the region. Thus, the vegetation indicator model becomes:

$$G_z = (NDV - NDVI_{\min}) / (NDVI_{\max} - NDVI_{\min})$$

Thus, the vegetation index in the mixed pixel is transformed into the surface vegetation coverage. ERDASIMAGE9.1 platform and Modeler were used to construct a quantitative conversion model of vegetation coverage. According to the spectral characteristics of pixels, vegetation coverage was statistically classified and graded according to $0\% \sim 5\%, 5\% \sim 20\%, 20\% \sim 50\%$, and $50\% \sim 100\%$.

4. Results and discussion.

4.1. Research on the correlation between vegetation index and precipitation. The correlation analysis of NDVI and precipitation in the study area in each month from 2015 to 2022 (Table 4.1) shows that precipitation has a strong lag effect on NDVI. The average of the two is the largest between the "precipitation of the month and the previous month." This is inconsistent with the correlation between the average precipitation of the previous month and the previous month, which is related to the natural conditions in the study area. Xi 'an is the primary water source in the four pilot zones [16]. The degree of correlation with the other three regions is small. And they have little correlation with precipitation (Table 4.1).

Through the linear regression of NDVI and the average data of "precipitation in the current month and the previous month," the correlation between the two is obtained in Yan 'an area [17]. It is followed by Yulin and Ankang, Xi 'an is the lowest, and there is a big difference between the fitting results and the ideal conditions that increase with the elevation. The reason is probably because the Yulin area is mainly desert, and the

Table 4.1: *Correlation between vegetation index and precipitation in Yulin, Yan 'an, Xi 'an and Ankang.*

	C	C P1	C P2	C P3
Yulin	0.619	0.771	0.767	0.668
Yan'an.	0.798	0.853	0.782	0.649
Xi 'an	0.202	0.286	0.068	-0.086
Ankang	0.535	0.569	0.477	0.310

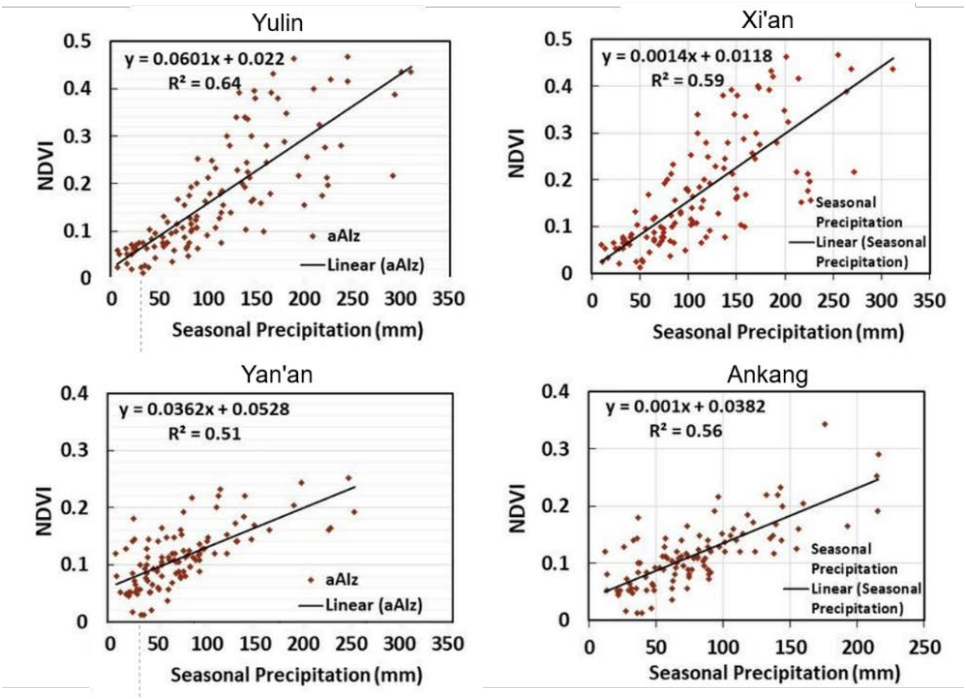

Fig. 4.1: *Linear correlation analysis of vegetation index and precipitation: Yulin, Yan 'an, Xi 'an, Ankang.*

relationship between them is weakened due to decreased vegetation coverage. The extensive irrigation area in Xi 'an reduces its sensitivity to rainfall. The average annual rainfall in Ankang is more than 800 mm. Natural precipitation has little effect on ground vegetation. Therefore, Yan 'an has become a typical area for studying the impact of green landscapes in this region (FIG. 4.1).

4.2. NDVI change analysis. The NDVI of the Ankang region from 2016 to 2022 (FIG. 4.2) showed a significant upward trend every month, and the area increased by 94.3% from July to September. In addition, the southeast and the north are the important distribution areas of grassland and dry land, while the southwest is the smallest distribution area of forest and shrubs [18]. The August NDVI growth rate reached 99.12%, with July to September the same. In October, NDVI increased significantly in all provinces and regions, but the differences among regions decreased. In the north, the increase rate was significantly lower than that from July to September, but in the west, the highest value was still located in the southeast, and in the middle, there was a band of low-value area of NDVI, indicating that the water distribution in this region was closely related to the change of irrigation area.

NDVI has increased significantly each month, which is 1.45 and 1.41 in October, August and July-September 2022 (Figure 4.3). The spatial variation trend of NDVI in October showed that the highest point of the NDVI curve from 2016 to 2022 was from high to low, and the number of patches at the highest point showed a

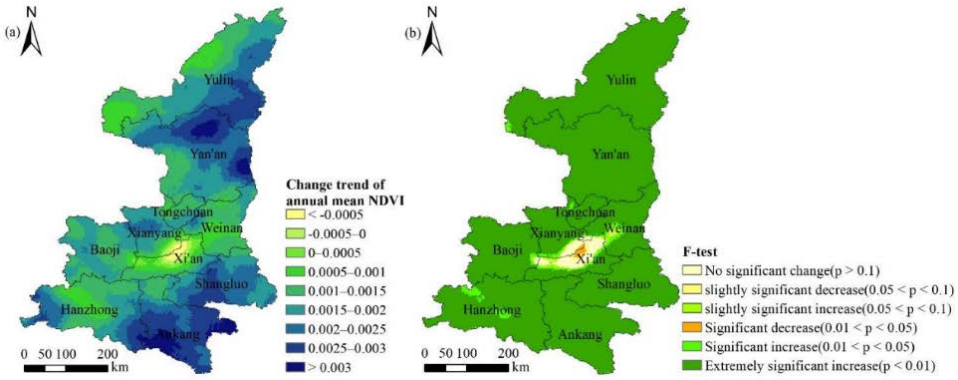

Fig. 4.2: *Spatial distribution of NDVI growth in Ankang from 2016 to 2022.*

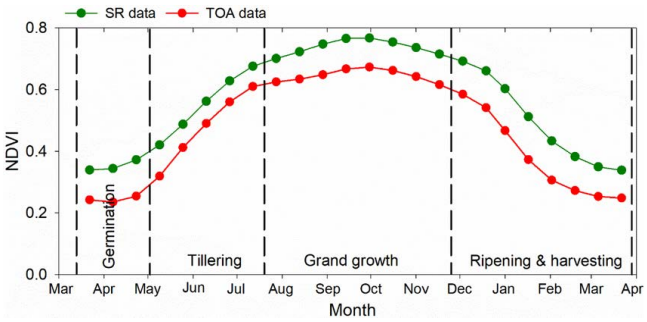

Fig. 4.3: *Quantitative distribution of NDVI changes from July to September, August and October in Ankang from 2016 to 2022.*

decreasing trend, which indicated that the coverage of surface grassland, shrub and forest land was constantly improving, and there was a decreasing trend among different regions [19]. Under the influence of natural and human factors, the vegetation coverage of agricultural land increased significantly from 2016 to 2022. However, the analysis of NDVI and corresponding precipitation data in October shows that the variation amplitude of NDVI during 2018-2022 is not uniform, especially during 2018-2022. Therefore, it is suggested that precipitation cannot explain the variation of NDVI well. In addition, different underlying surface conditions have different effects on NDVI.

4.3. Effect analysis of garden vegetation coverage. The changing trend of the vegetation index in the Ankang region from July to October 2015 to 2022 shows that human activities have an essential impact on the growth of the vegetation cover index (Figure 4.4). NDVIC increased the most in July, from 0.31 in 2015 to 0.35 in 2022, due to the greening of the region, which has increased the vegetation coverage per unit area by returning some dry fields that existed as bare soil during the cultivation period to woodland/scrub/grassland. NDVIC volatility increased in August and September but was not as large as in July. NDVIC of the forest/irrigation/grass composite system increased significantly in October, indicating that the forest/irrigation/grass composite area will increase rapidly from 2015 to 2022, which is also an objective reflection of the impact of landscape plants on the ecosystem. However, very few observational data available at present cannot show the location of new forests/grasslands in landscape greening projects. Moreover, the productivity of the farmland ecosystem is improved, which makes the NDVIC value of the farmland ecosystem continue to rise. Because of the limitations of the data, people could not identify them.

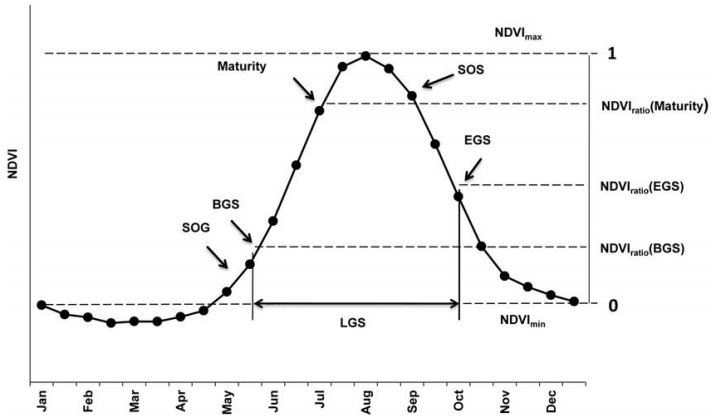

Fig. 4.4: *Changes of NDVIC value in Ankang City from 7, 8, 9, and 10 2015 to 2022.*

5. Conclusion. NDVI is an effective method to study vegetation distribution's spatial and temporal trends. The NDVI variation index excluding precipitation was established based on previous studies on the relationship between NDVI and precipitation. The paper will take Ankang as a case to evaluate the effectiveness of the project quantitatively. The results show that (1) there is a significant correlation between NDVI and precipitation, but there is a lag in the response to rainfall, in which the lag time of Yulin area, Yan 'an area, Xi 'an area and Ankang area is one month. The precipitation is the average precipitation in the current and previous months. The correlation also increases as the latitude increases from low-value to high-value regions. (2) NDVI of Ankang City showed a significant upward trend from 2016 to 2022, and the most significant trend was from 2002 to 2022, mainly in the dry land and grassland in the southeast of the city. There are natural and humanistic reasons for this phenomenon, and the humanistic reasons are caused by landscape greening and other reasons. The Ankang Greening project has achieved remarkable results, and the number of NDVICs in October 2015-2022 has significantly increased, which is reflected in this goal. (3) The specific location and scope of green land are accurately located according to the correlation between NDVI and rainfall to realize better the quantitative evaluation of the engineering effect of landscape green land based on adding meteorological observation stations.

6. Acknowledgement. The project is supported by Research on the Construction of Ideological and Political System for Landscape Architecture Majors in Local Applied Undergraduate Colleges, 230713280207219; Investigation and Restoration of Plant Community Diversity in the Yinghu Reservoir Area of Ankang, 202311397023; Breeding and Demonstration Promotion of Local High Quality Germplasm Resources in Xinxi Village, Minzhu Town, 2023AYXCZX01.

REFERENCES

[1] Hussain, S., & Karuppannan, S. (2023). Land use/land cover changes and their impact on land surface temperature using remote sensing technique in district Khanewal, Punjab Pakistan. Geology, Ecology, and Landscapes, 7(1), 46-58.
[2] Macarringue, L. S., Bolfe, É. L., & Pereira, P. R. M. (2022). Developments in land use and land cover classification techniques in remote sensing: A review. Journal of Geographic Information System, 14(1), 1-28.
[3] Dhanaraj, K., & Angadi, D. P. (2022). Land use land cover mapping and monitoring urban growth using remote sensing and GIS techniques in Mangaluru, India. GeoJournal, 87(2), 1133-1159.
[4] Tariq, A., & Mumtaz, F. (2023). Modeling spatio-temporal assessment of land use land cover of Lahore and its impact on land surface temperature using multi-spectral remote sensing data. Environmental Science and Pollution Research, 30(9), 23908-23924.
[5] Abijith, D., & Saravanan, S. (2022). Assessment of land use and land cover change detection and prediction using remote sensing and CA Markov in the northern coastal districts of Tamil Nadu, India. Environmental Science and Pollution Research, 29(57), 86055-86067.

[6] Tolche, A. D., Gurara, M. A., Pham, Q. B., & Anh, D. T. (2022). Modelling and accessing land degradation vulnerability using remote sensing techniques and the analytical hierarchy process approach. Geocarto International, 37(24), 7122-7142.
[7] Zeren Cetin, I., Varol, T., Ozel, H. B., & Sevik, H. (2023). The effects of climate on land use/cover: a case study in Turkey by using remote sensing data. Environmental Science and Pollution Research, 30(3), 5688-5699.
[8] Pande, C. B. (2022). Land use/land cover and change detection mapping in Rahuri watershed area (MS), India using the google earth engine and machine learning approach. Geocarto International, 37(26), 13860-13880.
[9] Chatterjee, U., & Majumdar, S. (2022). Impact of land use change and rapid urbanization on urban heat island in Kolkata city: A remote sensing based perspective. Journal of Urban Management, 11(1), 59-71.
[10] Kamaraj, M., & Rangarajan, S. (2022). Predicting the future land use and land cover changes for Bhavani basin, Tamil Nadu, India, using QGIS MOLUSCE plugin. Environmental Science and Pollution Research, 29(57), 86337-86348.
[11] Degerli, B., & Çetin, M. (2022). Using the remote sensing method to simulate the land change in the year 2030. Turkish Journal of Agriculture-Food Science and Technology, 10(12), 2453-2466.
[12] Cheng, C., Zhang, F., Shi, J., & Kung, H. T. (2022). What is the relationship between land use and surface water quality? A review and prospects from remote sensing perspective. Environmental Science and Pollution Research, 29(38), 56887-56907.
[13] Mariye, M., Mariyo, M., Changming, Y., Teffera, Z. L., & Weldegebrial, B. (2022). Effects of land use and land cover change on soil erosion potential in Berhe district: A case study of Legedadi watershed, Ethiopia. International Journal of River Basin Management, 20(1), 79-91.
[14] Bayaraa, B., Hirano, A., Purevtseren, M., Vandansambuu, B., Damdin, B., & Natsagdorj, E. (2022). Applicability of different vegetation indices for pasture biomass estimation in the north-central region of Mongolia. Geocarto International, 37(25), 7415-7430.
[15] Pan, X., Wang, Z., Gao, Y., Dang, X., & Han, Y. (2022). Detailed and automated classification of land use/land cover using machine learning algorithms in Google Earth Engine. Geocarto International, 37(18), 5415-5432.
[16] Saralioglu, E., & Gungor, O. (2022). Semantic segmentation of land cover from high resolution multispectral satellite images by spectral-spatial convolutional neural network. Geocarto International, 37(2), 657-677.
[17] Wang, L., Wang, J., Liu, Z., Zhu, J., & Qin, F. (2022). Evaluation of a deep-learning model for multispectral remote sensing of land use and crop classification. The Crop Journal, 10(5), 1435-1451.
[18] Rahman, M. T. U., & Esha, E. J. (2022). Prediction of land cover change based on CA-ANN model to assess its local impacts on Bagerhat, southwestern coastal Bangladesh. Geocarto International, 37(9), 2604-2626.
[19] Hashim, B. M., Al Maliki, A., Sultan, M. A., Shahid, S., & Yaseen, Z. M. (2022). Effect of land use land cover changes on land surface temperature during 1984–2020: A case study of Baghdad city using landsat image. Natural Hazards, 112(2), 1223-1246.

Edited by: Hailong Li
Special issue on: Deep Learning in Healthcare
Received: Mar 5, 2024
Accepted: Apr 21, 2024